Electronic Supplementary information

Cumulative effects of doping on Sn_3O_4 structure and electrode performance for rechargeable sodium-ion batteries

Ujjwala P Chothe[a], Anuradha A Ambalkar[a], Chitra K Ugale[a], Milind V Kulkarni[a], Bharat B Kale*[a]

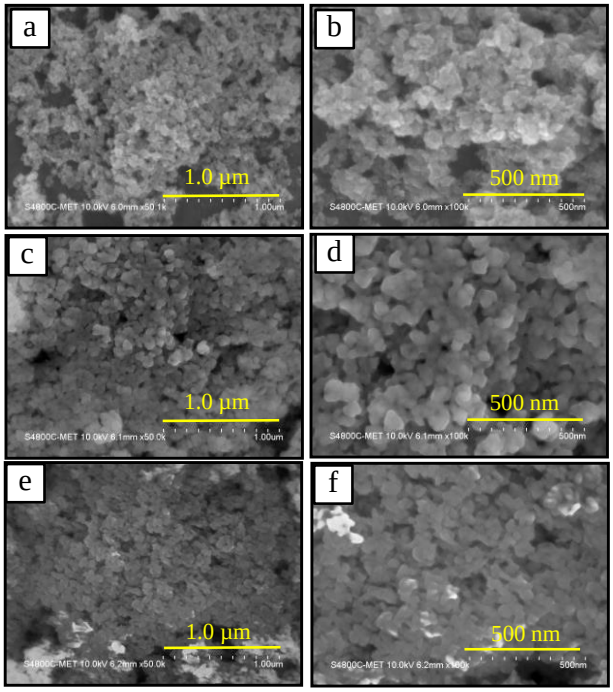

Figure S1: FESEM images of Sn_3O_4samples (a, b) SF-1 (c,d) SF-2(e,f) SF-4 at low and high magnifications

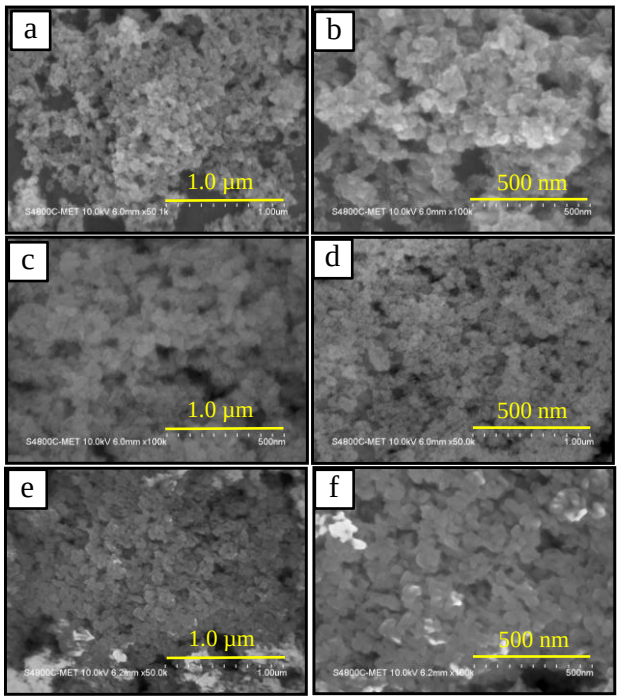

Figure S2: FESEM images of Sn_3O_4samples (a, b) SBF-1 (c,d) SBF-3 (e,f) SBF-4 at low and high magnifications

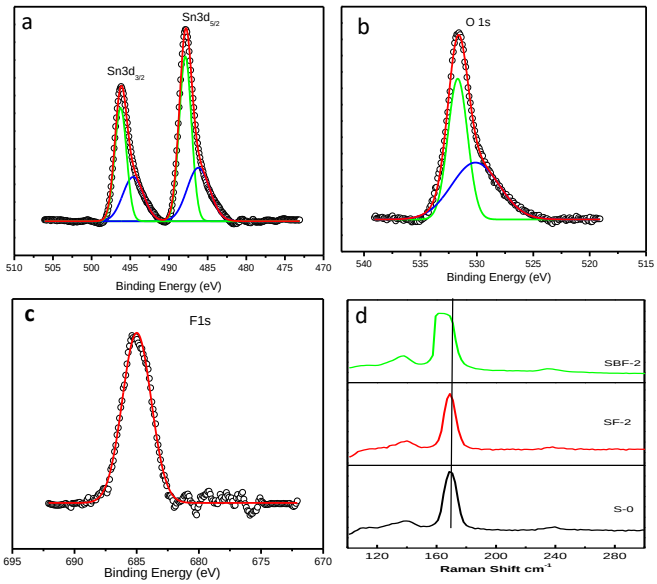

Figure S3: XPS spectra of F@Sn_3O_4 (SF-2) (a) Sn (b) O (c) F (d) Zoomed Raman spectra of S-0, SF-2 and SBF-2

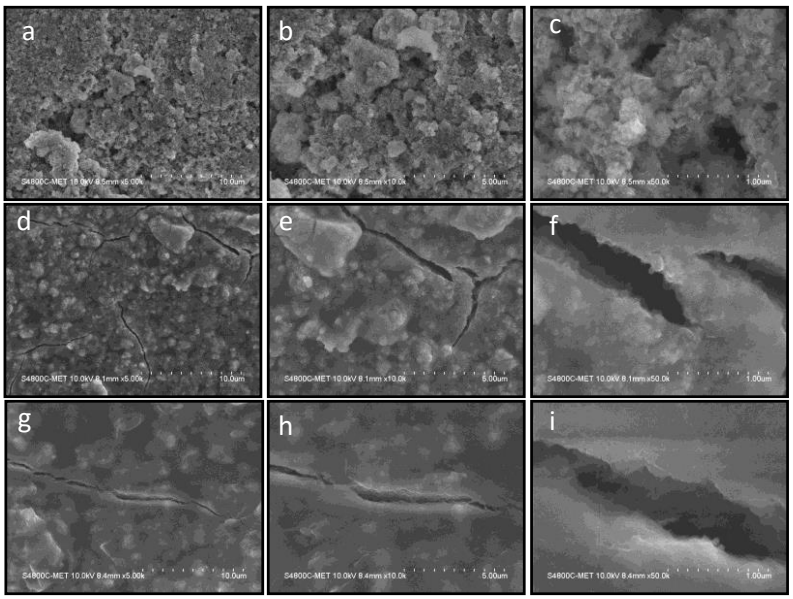

Figure S4: FESEM images of Sn3O4 samples after cycles (a, b,c) S-0 (d, e, f) SF-3 & (g,h,i) SBF-2 at low and high magnifications

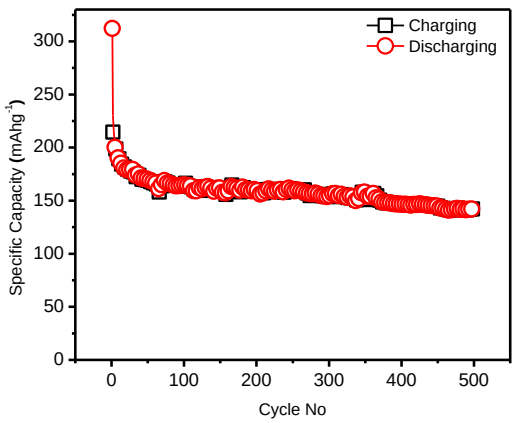

Figure S5: The cycling performance of SBF-2 at 1000 mAg^{-1} in a voltage range 0.01 to 3.0 V

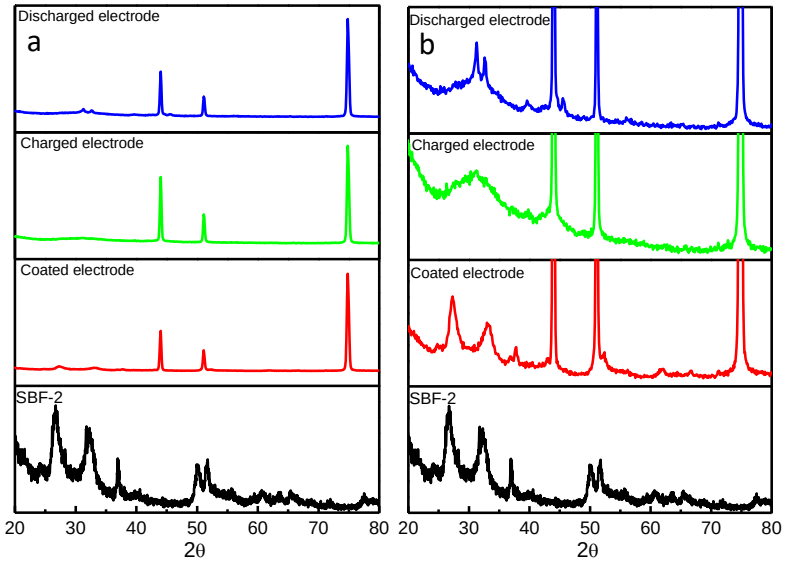

Figure S6: (a) XRD of Sn_3O_4 (SBF-2) Electrode Coated electrode , Charged electrode & Discharged electrode (b) Zoomed XRD

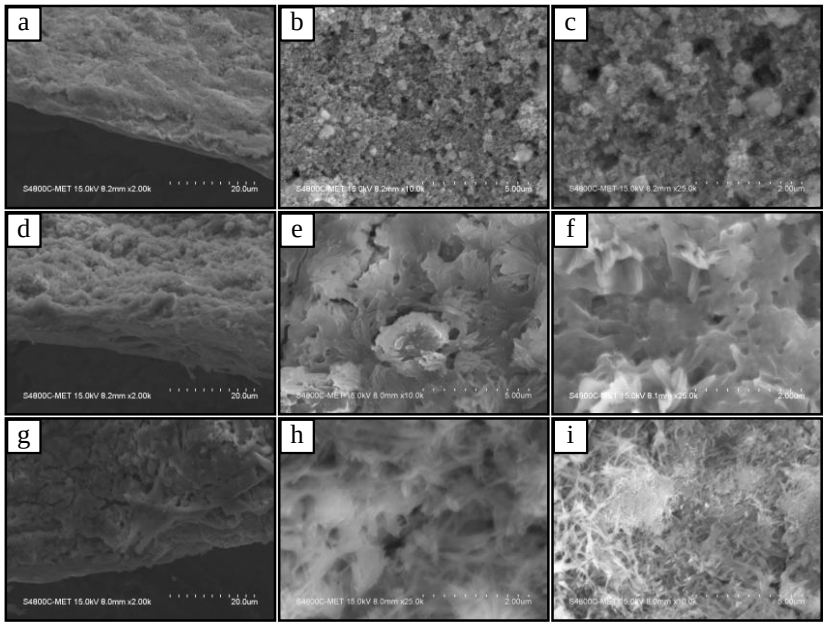

Figure S7: FESEM images of Sn_3O_4 (SBF-2) at low and high magnifications (a, b, c) Coated electrode (d, e, f) Charged electrode & (g, h, i) Discharged electrode

Material synthesis of $Na_3V_2(PO_4)_3$-C (NVP-C):

All the reagents were analytical pristine grade and used without further purification. The $Na_3V_2(PO_4)_3$-C was synthesized by employing a sol–gel technique using the NaOH (3 mmol), V_2O_5(1 mmol), $NH_4H_2PO_4$ (3 mmol), and citric acid (3 mmol) as precursors. All precursors dissolved in 100 ml distilled water. The mixture was stirred for 4 h, which resulted in a clear sol. The prepared sol was then kept in an oven at 120°C for drying to completely remove water content from it. After, it was ground in a mortar and pestle and subjected to a first sintering at 350°C for 3 h in the presence of flowing argon. The sample was then cooled to room temperature, ground again using a mortar and pestle, and subjected to a second sintering treatment at 800°C for 8 h, under argon, to obtain the desired material.

Figure S8a shows a XRD and FESEM images of as synthesized NVP-C. All reflections can be indexed to the typical $Na_3V_2(PO_4)_3$-C structure. The XRD pattern shows distinct peaks and these diffraction peaks of NVP-C is in good agreement with the crystallographic structure of rhombohedral with R-3c space group. All the peaks can be indexed the reference JCPDS No. 01-078-7289, without any additional impurity peaks. The high and low-magnification FESEM images depicts that the microstructures are in size ~1µm shown in fig S8 b,c. In addition, these microscopic structures also suggest the topographically uneven surface. Citric acid acted as a chelating agent and simultaneously a carbon source. The coating of carbon in shell structures is because of citric acid, which during the annealing process, may lead to the porosity in lieu of burnt organic precursors. This porous microstructure may assist in sodium ion diffusion during ionic transport and thus may lead to enhanced ionic diffusivity.

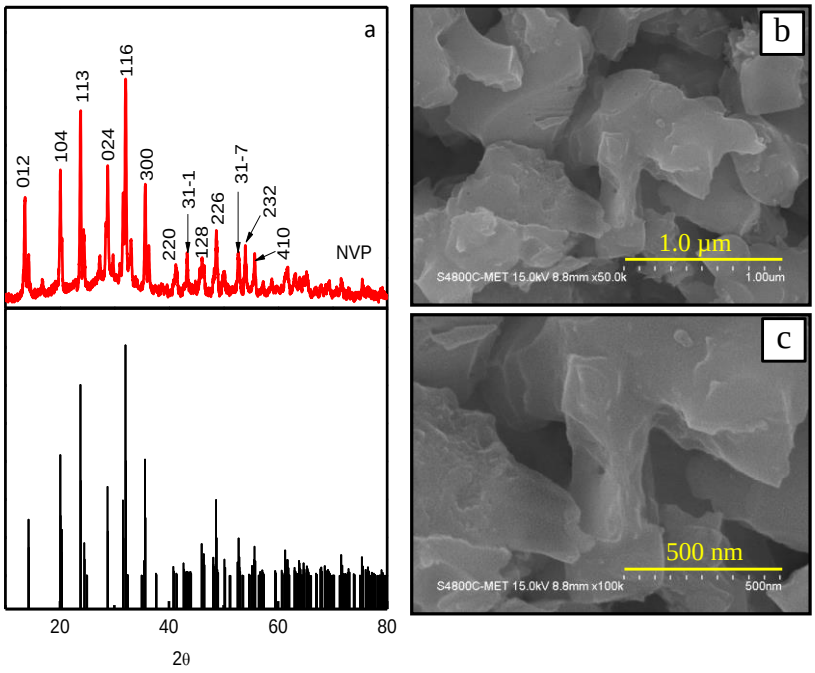

Figure S8: (a) XRD of as synthesized NVP (b, c) FESEM images of NVP sample at low and high magnifications

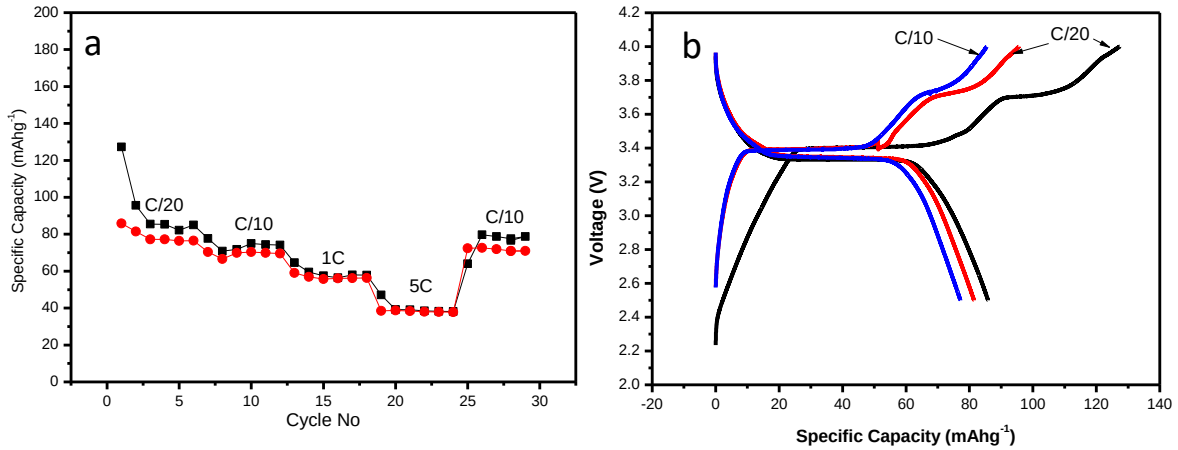

Figure S9: (a) The rate performance of $Na_3V_2(PO_4)_3$ and (b) The initial discharge-charge profiles at C/ 20 in a voltage range 2.5 to 4.0 V

Table S1: Comparison of the Sn based nanocomposites for their electrochemical performance

No	Current density	Reversible Capacity $mAhg^{-1}$ (at initial Cycle)	Rate performance capacity($mAhg^{-1}$) @current density (cycle)	Reference
1	0.2 C	790	515 @0.1C (50)	Yolk-shell Sn_4P_3@C [1]
2	0.03 Ag^{-1}	729	713@30 mAg^{-1} (70)	C@SnS/SnO_2@graphene [2]
3	0.05 Ag^{-1}	530	396@ 50 mAg^{-1} (150)	MoS_2@SnO_2@C [3]
4	20 mA g^{-1}	569	638 @20 mAg^{-1} (100)	SnO2@graphene [4]
5	0.2 C	748	326@ at 200 mAg^{-1}	Porous SnO_2 [5]
6	0.1 A g^{-1}	568	454@ 100 mA g^{-1} (200)	Sn/NS-CNFs@rGO [6]
7	0.2 A g^{-1}	493.6	415 @1000 mAg^{-1} (500)	Sn/C [7]
8	0.04 A g^{-1}	828	583@ 40 mAg^{-1} (200)	Sn/carbon nanocage [8]
9	0.1 C	808.19	776.26@0.1C (100)	Sn Nanofibers [9]
10	0.05 Ag^{-1}	400	308@ 200 mAg^{-1} (200)	SnO_2@void@C porous nanowires [10]
11	0.05 Ag^{-1}	223	137@ 100mAg^{-1} (400)	Sn/SnO nanosheets [11]
12	0.05 Ag^{-1}	399.4	118 @2Ag^{-1} (1200)	SnO/rGO [12]
13	0.1Ag^{-1}	1052	400 @ 1 Ag^{-1} (800)	Sn@SnO_2/CC [13]
14	0.05 Ag^{-1}	705	368.65 @200 mAg^{-1} (150)	P-F@Sn_3O_4 [14]
15	0.05 Ag^{-1}	732.8	396.60@200 mAg^{-1} (120)	**Present work**

Notes and references

1. J. Liu, P. Kopold, C. Wu, P. A. van Aken, J. Maier and Y. Yu, Uniform yolk–shell Sn 4 P 3@ C nanospheres as high-capacity and cycle-stable anode materials for sodium-ion batteries, *Energy & Environmental Science*, 2015, **8**, 3531-3538.
2. Y. Zheng, T. Zhou, C. Zhang, J. Mao, H. Liu and Z. Guo, Boosted charge transfer in SnS/SnO2 heterostructures: toward high rate capability for sodium-ion batteries, *Angewandte Chemie*, 2016, **128**, 3469-3474.
3. Z. Chen, D. Yin and M. Zhang, Sandwich-like MoS2@ SnO2@ C with high capacity and stability for Sodium/Potassium ion batteries, *Small*, 2018, **14**, 1703818.
4. D. Su, H.-J. Ahn and G. Wang, SnO 2@ graphene nanocomposites as anode materials for Na-ion batteries with superior electrochemical performance, *Chemical communications*, 2013, **49**, 3131-3133.
5. H. Bian, J. Zhang, M.-F. Yuen, W. Kang, Y. Zhan, Y. Denis, Z. Xu and Y. Y. Li, Anodic nanoporous SnO2 grown on Cu foils as superior binder-free Na-ion battery anodes, *Journal of Power Sources*, 2016, **307**, 634-640.
6. L. Luo, J. Song, L. Song, H. Zhang, Y. Bi, L. Liu, L. Yin, F. Wang and G. Wang, Flexible conductive anodes based on 3D hierarchical Sn/NS-CNFs@ rGO network for sodium-ion batteries, *Nano-Micro Letters*, 2019, **11**, 63.
7. Y. Liu, N. Zhang, L. Jiao, Z. Tao and J. Chen, Ultrasmall Sn nanoparticles embedded in carbon as high-performance anode for sodium-ion batteries, *Advanced Functional Materials*, 2015, **25**, 214-220.

8. S. Chen, Z. Ao, B. Sun, X. Xie and G. Wang, Porous carbon nanocages encapsulated with tin nanoparticles for high performance sodium-ion batteries, *Energy Storage Materials*, 2016, **5**, 180-190.
9. D.-H. Nam, T.-H. Kim, K.-S. Hong and H.-S. Kwon, Template-free electrochemical synthesis of Sn nanofibers as high-performance anode materials for Na-ion batteries, *ACS nano*, 2014, **8**, 11824-11835.
10. H. Li, L. Yang, J. Liu, S. Li, L. Fang, Y. Lu, H. Yang, S. Liu and M. Lei, Improved electrochemical performance of yolk-shell structured SnO2@ void@ C porous nanowires as anode for lithium and sodium batteries, *Journal of Power Sources*, 2016, **324**, 780-787.
11. F. He, Q. Xu, B. Zheng, J. Zhang, Z. Wu, Y. Zhong, Y. Chen, W. Xiang, B. Zhong and X. Guo, Synthesis of hierarchical Sn/SnO nanosheets assembled by carbon-coated hollow nanospheres as anode materials for lithium/sodium ion batteries, *RSC Advances*, 2020, **10**, 6035-6042.
12. X. Yang, H.-J. Liang, X.-X. Zhao, H.-Y. Yu, M.-Y. Wang, X.-J. Nie and X.-L. Wu, A sandwich nanocomposite composed of commercially available SnO and reduced graphene oxide as advanced anode materials for sodium-ion full batteries, *Inorganic Chemistry Frontiers*, 2020.
13. M. Liu, J. Huang, J. Li, L. Cao, Y. Zhao, M. Ma and K. Koji, Manipulating the stress of Sn in carbon structure to realize long-life high performance sodium ion battery anode material, *Journal of Alloys and Compounds*, 2020, 155177.
14. U. P. Chothe, A. A. Ambalkar, C. K. Ugale, M. V. Kulkarni and B. B. Kale, Synergy of a heteroatom (P–F) in nanostructured Sn3O4 as an anode for sodium-ion batteries, *Sustainable Energy & Fuels*, 2021, **5**, 2678-2687.